Protein Science (2000), *9*:1073–1084. Cambridge University Press. Printed in the USA.
Copyright © 2000 The Protein Society

A new model for 20-hydroxyecdysone and dibenzoylhydrazine binding: A homology modeling and docking approach

JEAN-MARIE WURTZ,[1] BENOIT GUILLOT,[1,3] JÉRÔME FAGART,[1] DINO MORAS,[1] KLAUS TIETJEN,[2] AND MICHAEL SCHINDLER[2]

[1]Laboratoire de Biologie Structurale, Institut de Génétique et de Biologie Moléculaire et Cellulaire, CNRS/INSERM/ULP, B.P. 163, 67404 Illkirch Cedex, C.U. de Strasbourg, France
[2]Department of Molecular Target Research, Agricultural Center Monheim, Bayer AG, D-51368 Leverkusen, Germany

(RECEIVED January 25, 2000; FINAL REVISION March 28, 2000; ACCEPTED April 6, 2000)

Abstract

The ecdysone receptor (ECR), a nuclear transcription factor controlling insect development, is a novel target for insecticides such as dibenzoylhydrazines with low environmental and toxicological impacts. To understand the high selectivity of such synthetic molecules toward ECR, two homology models of the *Chironomus tentans* ECR ligand-binding domain (LDB) have been constructed by taking as templates the known LBD crystal structures of the retinoic acid and vitamin D receptors. Docking of 20-hydroxyecdysone (20E) and dibenzoylhydrazines to the receptor suggests a novel superposition of the natural and synthetic molecules; the N-*tert*-butyl substituent of the dibenzoylhydrazines extends significantly beyond the 20E volume. Our ECR–LBD protein models rationalize how 20E and dibenzoylhydrazines interact with the ligand-binding pocket. The homology model complexes provide new insights that can be exploited in the rational design of new environmentally safe insecticides.

Keywords: dibenzoylhydrazine; docking; ecdysone; molecular modeling; nuclear receptor

Nuclear receptors (NRs) are a well-characterized superfamily of proteins containing over 150 members. Examples are steroid receptors and vitamin D receptors. Nuclear receptors act as transcription factors mediating between extracellular signals like hormones and transcriptional events (Gronemeyer & Laudet, 1995). The nuclear receptors are modular proteins, containing conserved domains for DNA-binding, ligand-binding (LDB), and other functions (Gronemeyer & Laudet, 1995). The three-dimensional (3D) structure of numerous LDBs are known and closely related (Moras & Gronemeyer, 1999). From this, a common fold for the ligand-binding pockets of all LDBs can be inferred (Wurtz et al., 1996).

Insect development, namely metamorphosis, is regulated by the steroid hormone ecdysone (Thummel, 1995, 1996) and its counteragent juvenile hormone. Ecdysone acts in the form of its active metabolite 20–hydroxyecdysone (20E) by binding to the ecdysone receptor (ECR). It is the heterodimeric complex composed of the ECR and the *ultraspiracle protein* (USP), both members of the NR family, which mediates the action of the hormone at the transcriptional level by binding to ecdysteroid response elements (Jones & Sharp, 1997). Since ecdysone is a hormone specific to invertebrates, the ECR is an interesting target for the development of new, environmentally safe insecticides.

Recently, the so-called dibenzoylhydrazines have been introduced by the Rohm & Haas company as insecticides (Wing et al., 1988). These compounds, like RH5992 (tebufenozide) and RH5849 (Fig. 1), exert their insecticidal effect by binding to the 20E binding site and activating ECRs permanently (Wing et al., 1988). The dibenzoylhydrazines have been found by classical screening without knowledge of their target. These insecticides do not exhibit any obvious structural analogy to ecdysone or 20E. The relationship of the dibenzoylhydrazines to 20E is still not satisfactorily understood, although there are several reports on structure activity relationships of dibenzoylhydrazines (Oikawa et al., 1994a, 1994b). Several attempts to relate the structure of dibenzoylhydrazines to the structure of 20E (Nakagawa et al., 1995b) based on the crystal

Reprint requests to: Jean-Marie Wurtz, Laboratoire de Biologie Structurale, Institut de Génétique et de Biologie Moléculaire et Cellulaire, CNRS/INSERM/ULP, B.P. 163, 67404 Illkirch Cedex, C.U. de Strasbourg, France; e-mail: wurtz@igbmc.u-strasbg.fr.

[3]Present address: Laboratoire de Cristallographie et Modélisation des Matériaux Minéraux et Biologiques, Faculté des Sciences, BP 239, 54506 Vandoeuvre-Lès-Nancy Cedex, France.

Abbreviations: ECR, ecdysone receptor; LDB, ligand-binding domain; 20E, 20-hydroxyecdysone; USP, ultraspiracle protein; hRARγ, human retinoic acid receptor; hVDR, human vitamin D receptor; LBP, ligand-binding pocket; QSAR, quantitative structure activity relationship; ECRra and ECRvd, ecdysone receptor model generated by taking as template the RAR and VDR crystal structures, respectively.

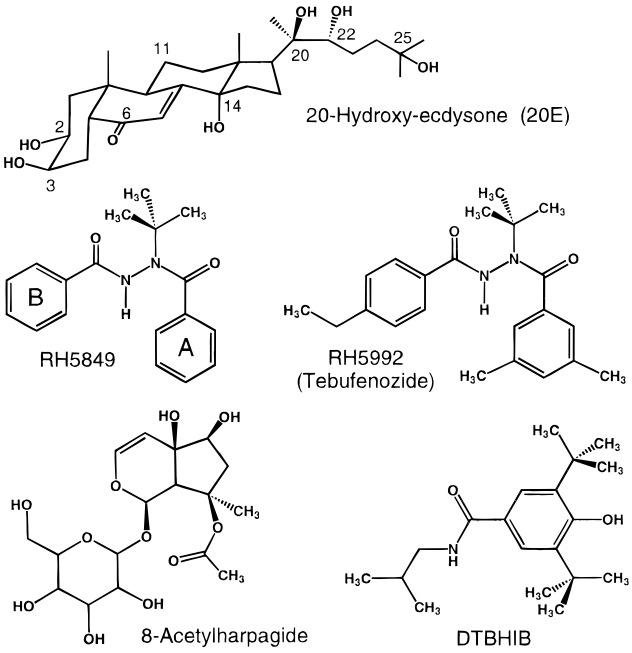

Fig. 1. Structures of the natural and synthetic ecdysone receptor ligands.

structures of RH5992 and RH5849 (Chan et al., 1990; Hsu et al., 1997) have been reported, as well as *ab initio* calculations (Reynolds & Hormann, 1996) of *N,N′*-dimethyl substituted diformylhydrazines. The latter family of molecules might serve as models for the dibenzoylhydrazines RH5849 and RH5992. In addition to the dibenzoylhydrazines, 8-O-acetylharpagide (Elbrecht et al., 1996) and DTBHIB (Mikitani, 1996) (Fig. 1) were discovered recently as nonsteroidal ligands for ecdysteroid receptors. As their affinities and biological activities are rather low, we will not consider these compounds further.

The present work describes homology models of an ecdysone receptor LBD constructed by taking the crystal structures of the human retinoic acid (hRARγ) and the human vitamin D (hVDR) receptor LBDs as templates (Renaud et al., 1995; Rochel et al., 2000). The homology model differences are discussed with respect to the overall fold, and the size and shape of their respective ligand-binding pocket (LBP). The 20E and RH5849 ligands have been docked in both models and discussed in the light of published data on the activity of various 20E or RH5849 derivatives. The superposition of 20E and the synthetic ligand in each model are unexpected and lead to novel ideas for designing new synthetic ECR ligands.

Results

Sequence alignment of ECRs with hRARγ and hVDR

The ECR members, of which 14 sequences are known, comprise six diptera (Koelle et al., 1991; Imhof et al., 1993; Cho et al., 1995; Hannan & Hill, 1997), four lepidoptera (Fujiwara et al., 1995; Kothapalli et al., 1995; Swevers et al., 1995; Jepson et al., 1996), one coleoptera (Mouillet et al., 1997), one orthoptera, one tick (Guo et al., 1998), and one crab (Chung et al., 1998). The ECR–LBD sequences exhibit a good conservation (54% residue identity) that is even higher within the diptera and lepidoptera subgroups (73 and 84%, respectively). The 11 helices (H1 to H12), of the alpha helical sandwich fold of NRs, are well identified (Fig. 2). These helices were used as the anchoring points in the model building process described below. The sequence alignment of the ECRs reveals strong amino acids conservation, especially in the NR signature region encompassing helices H3 and H4 (Wurtz et al., 1996). Furthermore, key residues in helix H1 are conserved among all ecdysone receptor members, especially Ile283, Leu286, Phe289, and Gln290 (in ECR *Chironomus tentans*, ctECR). They anchor H1 to the core of the protein and the AH motif common to the hRARγ (196-AH-197) and hVDR subgroup is replaced by the (FY)Q motif in ECRs (289-FQ-290 in ctVDR) (Thummel, 1995). Helix H12 exhibits the typical AF-2AD motif with the conserved Glu508 (in ctECR). A possibly important salt bridge interaction between this glutamate and Lys357 of H4 may be inferred from RAR and RXR data (Renaud et al., 1995).

Modeling of the ECR ligand-binding domain

Based on the assumption that NR-LBDs share a common 3D architecture (Wurtz et al., 1996), the 11–13 helices of hRARγ- or hVDR-LBD have been taken as templates for two different ctECR models (ECRra and ECRvd based, respectively, on the hRARγ and hVDR LBD crystal structures). The ctECR numbering will be used throughout the text if not otherwise mentioned (Imhof et al.,

Fig. 2 (*facing page***).** Sequence alignment of ecdysone nuclear receptor ligand-binding domains (LBD). The alignment includes ecdysone receptors from diptera (d), lepidoptera (l), coleoptera (co), orthoptera (o), and tick (t), insects and a crab (cr). The sequences of the human RARγ and VDR, for which crystal structures have been determined, are also included. The organism abbreviations are: aa: *Aedes aegypti* (d) (Cho et al., 1995); am: *Amblyomma amaricanun* (t) (Guo et al., 1998); bm: *Bombyx mori* (l) (Swevers et al., 1995); cc: *Ceratitis capitata* (d); cf: *Choristoneura fumiferana* (l) (Kothapalli et al., 1995); ct: *Chironomus tentans* (d) (Imhof et al., 1993); dm: *Drosophila melanogaster* (d) (Koelle et al., 1991); hs: *Homo sapiens*; hv: *Heliothis virescens* (l) (Jepson et al., 1996); lc: *Lucilia cuprina* (d) (Hannan & Hill, 1997); lm: *Lucusta migratoria* (o); ms: *Manduca sexta* (l) (Fujiwara et al., 1995); up: *Uca pugilator* (cr) (Chung et al., 1998); sc: *Sarcophaga crassipalpis* (l); tm: *Tenebrio molitor* (co) (Mouillet et al., 1997). The sequence numbering above and below the alignment are for the ctECR, the VDR, and the RARγ, respectively. Identical or similar residues in the whole alignment are highlighted in red and grey (the grouping used for similar residues is ILVM, FYW, TSCA, RK, DE, and QN). Identical residues among all ECR sequences are highlighted in green. Yellow and blue colored residues indicate conserved residues among diptera and lepidoptera, respectively. The secondary structure informations colored in green and blue correspond to the VDR and RARγ crystal structures, respectively. The residues in common to ECRvd and ECRra models closer than 4.5 Å to 20-hydroxyecdysone are indicated by red dots. Specific ones in the ECRvd and ECRra are in green and blue, respectively. The figure has been prepared using ALSCRIPT (Barton, 1993).

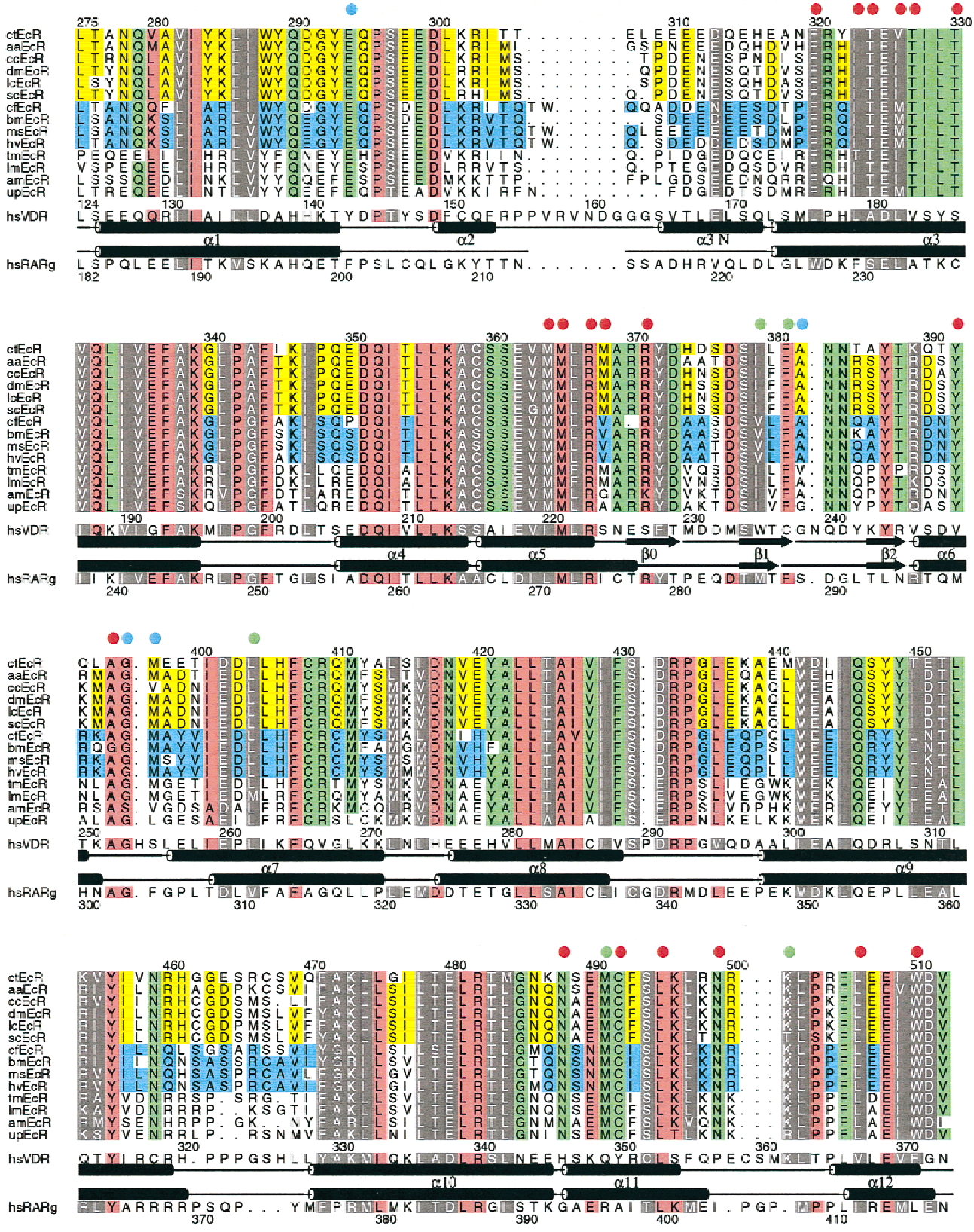

Fig. 2. *Caption on facing page.*

1993). From sequence comparison, the loop L1–3 connecting helices H1 and H3 is the more variable region in length. Indeed, VDRs are characterized in this region by a ~70 residue insertion as compared to ECRs and hRARγ. In the hVDR crystallization process, the authors used a truncated protein in which a part of the extension was deleted (residues Ser165 to Pro215) and was therefore omitted in the alignment. hRARγ and ctECR have only few differences in their loop length (in L8–9 and L9–10), whereas VDRs and ECRs are more divergent (a 7 residue deletion in L1-3, one in β1–β2, L6–7, and L11–12, and a three residue insertion in L9–10). Loop 1–3 is located on the protein surface in the vicinity of the LBP. Loops L6–7 and L11–12 are key regions lining the LBP and both could most likely affect the shape and size of the cavity. The loops in the ctECR models differing in length from those of the templates were taken as proposed by Modeller (Sali & Blundell, 1993).

The stereochemical parameters, as calculated with PROCHECK (Laskowski et al., 1993), show that more than 97% of the residues of the two models have the ϕ/ψ dihedral angles in the most favored or allowed regions of the Ramachandran plot and that side-chain dihedral angles are inside the range or better than the statistics derived from a set of crystal structures of at least 2.0 Å resolution. In addition, the program PROSAII (Hendlich et al., 1990) gives combined Z-scores (pair and surface potentials) of −7.7 and −8.5 for the ECRra and ECRvd models, values close to the range observed for hRXRα, hRARγ, and hVDR crystal structures (−7.4, −10.0, and −9.6, respectively). These results suggest that our models are of good quality despite the low sequence identity and are suitable for further analysis.

The ECR ligand-binding pocket

As in the LBD crystal structures, the ctECR-LBPs are delineated by the helices H5, H7, H11, and H12, the β-turn, and the loops L6–7 and L11–12 (Figs. 2, 3A,B). The calculated probe-occupied volume of 764 Å^3 (ECRra), and 840 Å^3 (ECRvd) as calculated with VOIDOO (Kleywegt & Jones, 1994) are consistent with the size of 20E [473 Å^3 as calculated with GRASP (Nicholls et al., 1991)]. The two cavities are lined by 23–24 residues, mostly hydrophobic. The polar residues, except one (Glu294 in ctECRra and Lys501 in ctECRvd), are common for the two models (Thr324, Thr327, and Thr330: H3; Arg367 and Arg371: H5; Tyr392: H6; Asn488, Cys492, and Asn499: H11). Both models were then used to dock the natural ligand 20-hydroxyecdysone (20E) and the synthetic agonist RH5849.

Docking of 20-hydroxyecdysone

The preformed pocket of both ctECR models are used to first manually dock the 20E using the probe-accessible and van der Waals volumes as guides, followed by restrained molecular dynamics calculations (see Material and methods).

Both LBPs exhibit a characteristic form with a bulky envelope and a shallow tube, but they are in an opposite orientation in the models. In the ECRvd model, the bulky part of the cavity is located near the β-sheet, whereas in the ECRra model it is close the helices H11 and H12. 20E is docked in the ligand-binding cavities according to the shape and size of the pocket and taking into account the putative hydrogen bonds the ligand forms with residues belonging to the LBP. In each model, 20E has the A-ring located in the bulky envelope and the tail in the shallow tube that results into head to tail orientation when both model complexes are compared (Fig. 3A,B).

In the homology models, each 20E polar groups are hydrogen bonded with residues lining the binding cavity (Table 1). As the ligands are in an inverted orientation in the two ECR models, the hydrogen bond network anchoring the ligand is inverted in both models (see Fig. 3A,B; Table 1). As an example, the C6-ketone moiety of 20E forms a hydrogen bond with Asn488 and the C25-hydroxyl group with Tyr392 in the ECRvd model, the reverse is observed in the ECRra model. Interestingly, in both models, the C14-hydroxyl group of 20E forms a hydrogen bond with Thr327 that is located in the middle of the binding pocket.

Conformational analysis and docking of RH5849

The crystal structures of the dibenzoylhydrazines RH5849 and RH5992 are known (Chan et al., 1990; Hsu et al., 1997). Their most prominent features are the almost orthogonal twists of the central hydrazine bonds and the *cis*-amide bond to the *tert*-butyl group (Figs. 1, 4). To explore their conformational flexibility, the rotational barrier of the central hydrazine bond (Θ) of RH5849 has been investigated by density functional theory (for details see Materials and methods). Two broad valleys are found for Θ, one between 35 and 135° and the other between −35 to −135°. Therefore, two classes of minimum energy structures have been taken into account. The conformations with negative torsion angles correspond to the crystal structure. The other conformation, designated as "rotated," can be obtained from the experimental structure by an ~180° rotation of the *trans*-amide moiety. Whereas the unsubstituted amide nitrogen of RH5849 remains planar, the *tert*-butyl nitrogen, though involved in an amide bond, is slightly pyramidal in each of the conformations investigated. Due to the influence of the NH-proton, the preferred orientation of the phenyl ring is 120 or 60° with respect to the carbonyl group of the *cis*-amide bond, while the other phenyl ring is almost coplanar (~20°) with respect to the carbonyl group of the *trans*-amide bond. The phenyl ring can almost be rotated freely when it is not substituted in the *ortho* position. The rotation of its counterpart is hindered to some extent by the effect of the NH-proton.

Fig. 3 (*facing page*)**.** 20-Hydroxyecdysone (20E) and RH5849 in the ligand-binding pocket. Stereo views showing the 20E and RH5849 ECR-LBD complexes based on the retinoic acid (ECRra; **A** and **C**, respectively) and the vitamin D (ECRvd; **B** and **D**, respectively) receptor crystal structures. 20E and RH5849 are depicted in blue with their oxygen atoms in red. The α-helices are drawn as ribbons and the β-sheet as arrows. The hydrogen bond network between the hormone and the protein is depicted by green dotted lines. (**E**, **F**) The superimposition of the 20E and the RH5849 ligands as obtained once docked to the ECR homology models based on the vitamin D and the retinoic acid receptor crystal structures, respectively, are shown. 20E is depicted in yellow and RH5849 in light blue. The oxygen and nitrogen atoms are colored in red and blue, respectively. The figures were produced with SETOR (Evans, 1993).

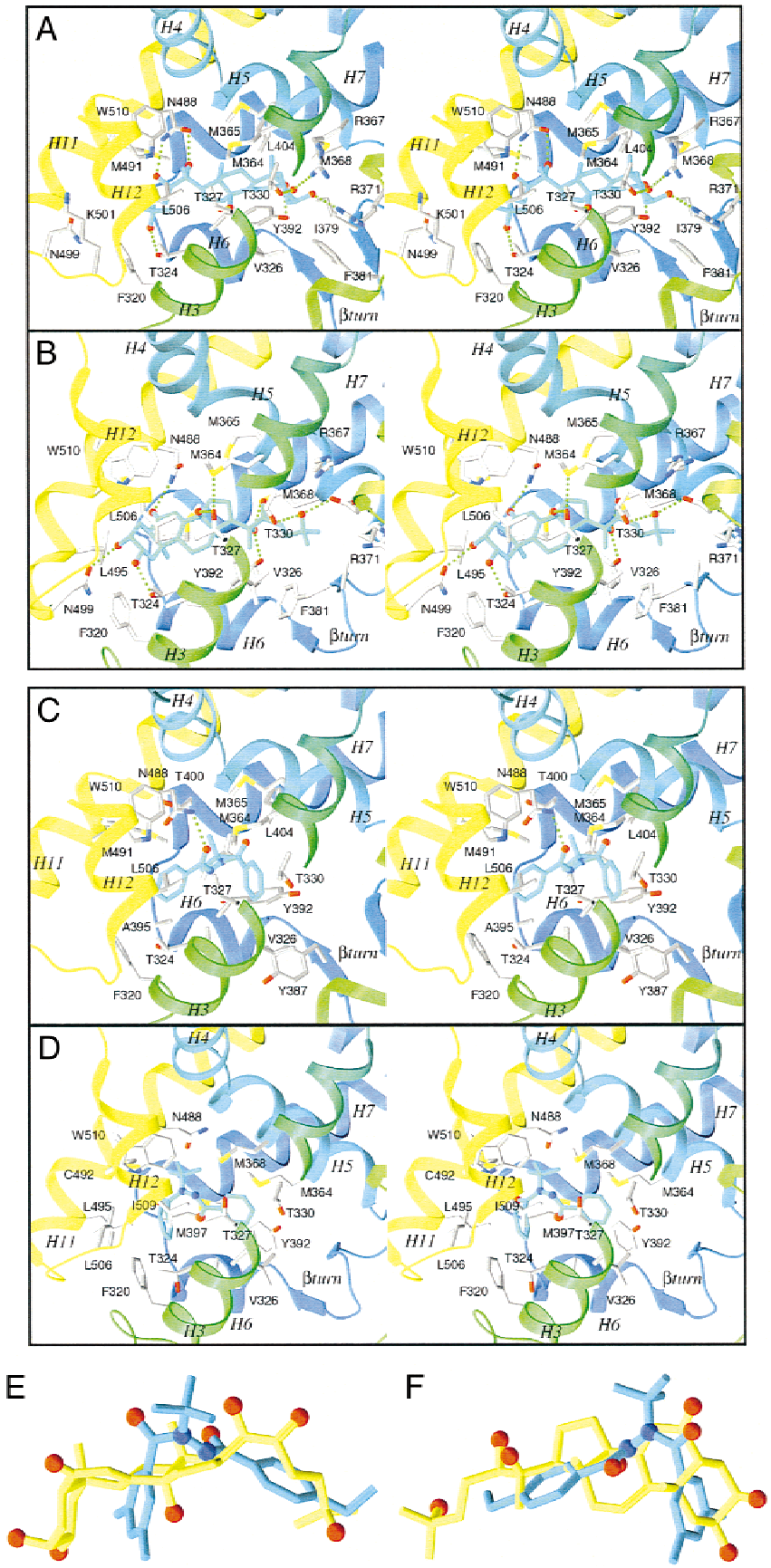

Fig. 3. *Caption on facing page.*

Table 1. *Hydrogen bond network between 20-hydroxyecdysone (20E) and the ctECR-LBD homology models based on the vitamin D (ECRvd) or the retinoic acid receptor (ECRra) crystal structures*[a]

	Hydrogen bond interaction partners												
Residues	Glu294	Thr324	Thr327	Thr330	Met364	Met364	Arg367	Met368	Arg371	Tyr392	Asn488	Asn488	Asn499
	Oδ	OH	OH	OH	C=O	S	NH_2	S	NH_2	OH	Cγ O	Cγ NH_2	Cγ NH_2
ECRra	25-OH	2-OH	14-OH	25-OH	22-OH	14-OH		20-OH		20-OH		6-C=0	3-OH
Distance (Å)	2.92	2.94	3.15	2.94	2.68	3.30		3.11		3.15		3.05	2.87
ECRvd		25-OH	14-OH	2-OH			2-OH		3-OH	6-C=0	20-OH	22-OH	
Distance (Å)		3.32	3.03	2.70			2.94		3.06	2.80	3.02	3.01	

[a]Distances are between heavy atoms.

A crystal-like and a "rotated" conformation of RH5849 were then docked manually into the ctECR-LBD models (Fig. 3C,D). From the overall shape of the binding niches and that of the dibenzoylhydrazines, it is clear that these—contrary to 20E and its homologs—are not able to fully occupy the space in the binding niches. From geometrical reasons there exists only one principal orientation of dibenzoylhydrazines in the LBD. The RH5849/ctECR complexes were then treated analogously to 20E/ctECRs.

As a result, in both models, the *tert*-butyl group of the dibenzoylhydrazines is located in the similar hydrophobic region (delineated by helices H5, H6, H7, and H11) occupied only partially by 20E. As for 20E, RH5849 adopts opposite orientations in both models and globally occupies the same volume. The bulky N-substituent can be favorably accommodated irrespective of which of the two principal conformations of the dibenzoylhydrazines we use. Nevertheless, the "rotated" conformer seems to fit better the shape of both cavities. In the ECRra model, the synthetic ligand is tightly packed (contacts to Gly396 and Cys492 with the A-ring), due to the smaller size of the binding cavity. In the ECRvd, the ligand has more room to fit. The ligand carbonyl (A–ring) is hydrogen bonded to Asn488 in the ECRvd model but not in the ECRra model.

Discussion

Despite a conserved fold observed for all NR–LBD crystal structures solved recently, major structural changes are revealed by a detailed comparison of their 3D structures. These changes affect dramatically the size and shape of the ligand-binding pocket. They are observed not only between structures of different NRs [ER (Brzozowski et al., 1997; Shiau et al., 1998; Tanenbaum et al., 1998), PPAR (Nolte et al., 1998), PR (Williams & Sigler, 1998), RAR (Renaud et al., 1995), RXR (Bourget et al., 1995), TR (Wagner et al., 1995), VDR (Rochel et al., 2000)] but also between complexes of the same receptor, as illustrated by the ER bound to natural and synthetic ligands (agonist or antagonist). RAR and VDR belong to the same phylogenetic subfamily as ECR (Gronemeyer & Laudet, 1995) and exhibit a similar sequence conservation with ECR (25%). Furthermore, VDR and ECR exhibit a A-, C-, D-ring in their ligands with a similar long and flexible hydrophobic tail, but differ in the B-ring that is open (seco-steroid) in vitamin D compounds (Dhadialla & Tzertzinis, 1997). Therefore, RAR and VDR structures have been used as structural templates to construct two distinct ECR models (ECRra and ECRvd). The two models do not include the F-region that is only moderately con-

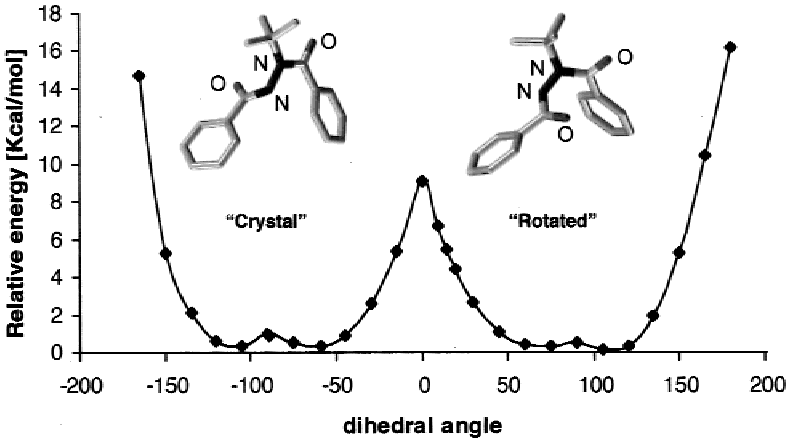

Fig. 4. Conformational analysis of RH5849. Diagram of relative energies of conformations obtained after rotation and fixation of the central N-N bond and minimization of the rest of the molecule. The left minimum correspond to a crystal-like conformation; the right minimum correspond to the "rotated" conformation. The latter has been found to fit best into the protein ligand-binding cavity.

served among the ECR sequences. This region is rather long for some of them (*Drosophila*) and may thus contribute to the stabilization of helix H12 together with the ligand, to modulate the transcriptional activity of these molecules. The homology models generated from these two templates exhibit rather different shapes of the ligand-binding cavity.

The docking of two representative ligands, the biological active compound (20E) and the synthetic ligand RH5948, results in an inverted orientation of the ligands in the two models. Experimental data on receptor activity in response to numerous 20E and RH5849 derivatives are exploited to further score the two models, and the superposition of 20E with RH5849 is discussed together with the divergence among residues lining the putative ligand–binding pocket of ECRs.

20-Hydroxyecdysone derivatives

The docking of 20E, the biological active compound, to the ECR models resulted in two orientations differing by 180° when the ECRra and ECRvd complexes are compared. In the RAR-based model, the ligand fits more tightly due to the smaller size of the cavity compared to the VDR model. To further corroborate either of the two models, the few available activity data on 20E derivatives (summarized in Fig. 5) are exploited to score each model (Table 2A). The score reflects the agreement between the experimental activity and the fitness of the ligand in the binding cavity upon substitution/deletion at given positions of the ligand. Mainly a hydroxyl group has been added at various positions of the steroid skeleton (5β-, 11α-, or 16β-OH; Fig. 5). The effect of these additions on the ligand activity (increase or decrease) can be explained for ECRra but not for ECRvd where steric contacts with the backbone are observed upon substitution. The presence of a 5β-OH, as in Polypodine B, would result in a steric contact with helix H5 in the ECRra model, which is in contradiction with its higher pI_{50} as compared to 20E. Furthermore, the 16β-OH substitution in the D-ring (Malacosterone) forms a hydrogen bond network with the 20- and 22-hydroxyl groups of the 17β-aliphatic chain. These H-bonds leave the preferred conformation of the chain unchanged (see Conformational analyses in Materials and methods). The 16β-OH of Malacosterone fits nicely in the LBP, in contradiction with the low activity of this ligand (Fig. 5). The introduction of a methyl group at position 24 (Makisterone) induces a different chain conformation due to unfavorable contacts with the 20-methyl group, or the 20- and 22-hydroxyl moieties. The altered chain conformation either decreases the activity of 20E derivatives with the 24(S) isomer or leaves the activity unchanged with the 24(R) isomer. This behavior is only partially explained by both models and slightly better by the ECRvd. The presence of the 20-hydroxyl group strongly enhances the activity of the molecule, in both models a hydrogen bond exists between this group and residues lining the cavity (Asn488 or Thr392 in ECRvd and ECRra, respectively). The removal of the 25-hydroxyl moiety, which increases the activity of the ligand, as in Ponasterone and Muristerone, disrupts a hydrogen bond network in ECRra in contradiction

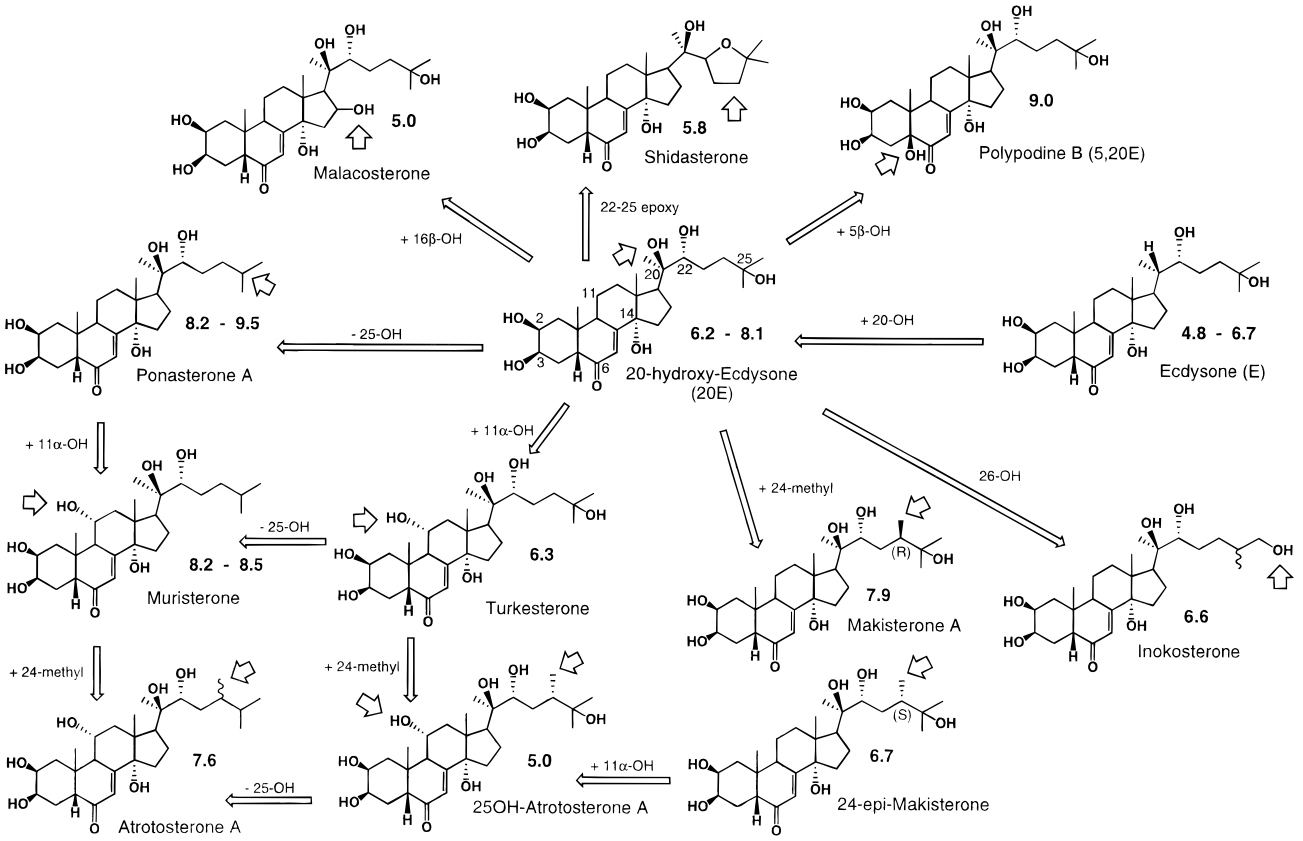

Fig. 5. Structures of 20-hydroxyecdysone derivatives and their diptera biological activities. pI_{50} values are from different assays (for sources see Table 3). The underlined values are for Drosophilia B_{II} based assay (Harmatha & Dinan, 1997).

Table 2. *Scoring of the ecdysone receptor complexes based on ligand binding data of 20-hydroxyecdysone (20E; see Fig. 6 and Table 3) and RH5849 (Thummel, 1996; Lafont, 1997) derivatives* [a]

A. 20E derivatives

	Model scores	
	ECRra	ECRvd
20E	++	+++
Ponasterone A (−25-OH)	−	+++
C24-methyl derivatives (R)	−	+++
C24-methyl derivatives (S)	++	+++
Inokosterone	++	+++
11αOH-derivatives	+	+++
Malacosterone (16β-OH)	+++	−
Polypodine B (5β-OH)	+++	−

B. RH5849 derivatives

	Activity		Model scores	
	Higher	Lower	ECRra	ECRvd
A-ring ortho	F, Cl, Br, I, Me	Et, OMe, Ph	+++	+++
A-ring meta	F, Cl, Br, I, Me	NO_2, CN, OMe	++	+++
A-ring para	F, Cl	Br, Me, t-Bu, Ph	−	+++
B-ring ortho		All	+++	+++
B-ring meta	F	Others	+	+
B-ring para	F, Cl, Br, I, CF_3, Et, i-Pr, t-Bu	Ph, CN, NO_2	−	+

[a] A scoring is given for the ECR-LBD homology models based on the vitamin D (ECRvd) and the retinoic acid receptor (ECRra) crystal structures for the (**A**) 20E and (**B**) RH5849 derivatives (the scoring is done by manual inspection, see Material and methods).

with its enhanced efficiency. In the ECRvd model, this deletion disrupts a hydrogen bond (Thr324) and relieves steric contacts with the nearby residues (e.g., Phe320; 3.2 Å). So both models are only partially in agreement with the experimental activity data, suggesting that specific spatial arrangements can be expected in the ECR structure similar to the differences observed between the RAR and VDR crystal structures.

RH5849 derivatives

In a manner similar to the 20E derivatives, the numerous Quantitative Structure Activity Relationship (QSAR) studies published on the dibenzoylhydrazine are used to score the fitness of the RH5849 derivatives in both orientations (Table 2B). Substitution by small groups on any of the benzoyl ring improves or leaves the ligand activity unchanged, except for the meta position of the B-ring (Table 2B). The data, summarized in Table 2B, reveal that the ECRvd model accounts well for the biological activity of the RH5849 derivatives, especially with substituents in the ortho and meta position of the A-ring where the ligands can only accommodate substituents like iodine or methyl. In contrast, the ECRra model would predict the opposit effect, which justifies its low score shown in Table 2B. In the case of the B-ring, the two models differ significantly in the para position where again with the ECRra model the opposite effect is predicted. A substitution in para of the B-ring by a cyanide group is allowed in this model, whereas such a substituent decreases the activity.

Based on the QSAR data available for the A- and B-ring of RH5849, the ECRra model is less efficient in explaining the activity profile of the substituted compounds. Nevertheless, it is worth to note that despite the previous differences, the two models suggest a similar location of the *tert*-butyl group. The presence of this group has been shown to confer a high ecdysone-like activity. In the homology models, the *tert*-butyl group forms extensive van der Waals contacts with the protein and fits nicely in a groove that is not occupied by the 20E molecule. Moreover, this bulky substituent locks the ligand in the pocket and prevents any displacement. Larger groups (an ethyl-2-cyclohexane) still exhibits a similar activity. For these substitutents, the LBP might have to adapt and require that the loop L6-7 be displaced to fit in the binding cavity. Small substituents (a methyl group) at this position dramatically decrease the activity of the synthetic ligand. This is due most likely to the fact that small substituents induce the *trans*-amide conformation and hence change the molecule's overall shape (Reynolds & Hormann, 1996).

Superposition of 20E and dibenzoylhydrazines

There exist several attempts to generate pharmacophore models for ecdysone agonists. The situation was complicated by the fact that, in addition to the hitherto unknown binding niche of the ecdysone receptor, there is no similarity between ecdysone and the hydrazines, and even no pattern of functional groups that could be used as anchor points in space. While classical studies do not suffer from these shortcomings, modern 3D approaches like CoMFA do (Cramer et al., 1989). As long as one does not attempt to develop a single model for both steroid and nonsteroid classes of agonists, simple superpositions of core structures might be sufficient. It is,

however, not satisfying to have two models for compounds that are known to bind at the same binding site. Therefore, several groups have developed combined models (Mohammed-Ali et al., 1995; Nakagawa et al., 1995b; Qian, 1996; Shimizu et al., 1997). But none of these predicted the superimposition suggested by the docking of the ligands (20E and RH5849) in the ECR models, and this despite the inverted orientation of the 20E and RH5849 in the binding cavity when the ECRra and ECRvd complexes are compared (Fig. 3E,F). In both models, the planes of the 20E A-ring and the A-ring of RH5848 (next to N-*tert*-butyl; Fig. 1) are roughly parallel, whereas the other phenyl ring (B-ring) superimposes with the beginning of the steroid aliphatic chain. Nevertheless, in the ECRvd the dibenzoylhydrazine and the 20E molecules are shifted whereas in the ECRra the A-rings almost superimpose (Fig. 3E,F). No counterpart in 20E is found for the *tert*-butyl group of the dibenzoylhydrazines that is located in the same groove of the ligand-binding cavity of the ECR-LBD homology models.

Differences among arthropod ECRs

The residue differences in the ligand-binding cavity observed for ECRs from different species (Fig. 2) do not affect the RH5849 activity (Table 3). In contrast to RH5849, the phenyl substituted dibenzoylhydrazine RH5992 (Fig. 1) is biologically more active on lepidoptera than on diptera and coleoptera. Interestingly, the two later groups present three divergent residues lining the binding pocket, Val326, Met368, and Ile379, as in *C. tentans* (Val326 is an isoleucine in all other diptera and coleoptera). These residues are replaced by a methionine and two valine residues, respectively, in lepidoptera. Especially the presence of a valine or isoleucine at position 326, in diptera and coleoptera, generates steric contacts between the γ-methyl group of these residues and the C5-methyl group of the RH5992 A-ring in the ECRvd complex or the B-ring C4-ethyl moiety in the ECRra complex, which most likely account for the lower activity in these species. It has also been shown that the ECR of *Anthonomus grandis* (coleoptera), for which the sequence is only partially known, exhibits a rather low affinity for RH5992 [$10^{-4.9}$ M (Dhadialla & Tzertzinis, 1997)]. The sequence comparison reveals a mutation for one of the residues lining the LBP, T327A (Dhadialla & Tzertzinis, 1997). Such a mutation disrupts the hydrogen bond observed between Thr327 and the *trans*-amide carbonyl moiety of the dibenzoylhydrazines. Furthermore, the present models would also predict lower affinities of dibenzoylhydrazines towards the ECR of *Tenebrio molitor* (coleoptera) (Mouillet et al., 1997) due to two significant residue changes in the binding cavity, I323T and A382V (see Fig. 2), which would most likely affect the contacts with any of the dibenzoylhydrazines phenyl rings and hamper the ethyl substituent of RH5992, respectively.

Since neither sequences nor binding data from completely resistant insects are known, it is hard to discuss the possibility of differences in the ligand-binding pockets of these insects. The mutation known in *A. grandis* might explain the lower affinity of RH5992 to the ECR of this insect. Nevertheless the strong conservation of the ligand-binding pocket residues in two noninsects, the tick *Amblyomma americanum* (Guo et al., 1998) and the crab *Celuca pugilator* (Chung et al., 1998), suggests that other factors than the structure of the ECR ligand-binding pocket also may determine the biological spectrum of the dibenzoylhydrazines.

Conclusion

The present ECR homology models reveal the conserved residues most likely involved in the specific binding of 20E and RH5849 derivatives. Only a few of them differ in the ligand-binding pocket accounting most likely for the different biological activity observed for synthetic ligands among various ECR species. Based on the experimental data currently available for the activity of 20E derivatives upon binding to ECRs and the structural differences observed among NR-LBDs, the present study cannot select unambiguously one of the two orientations of 20E identified in the ECR models (by taking the retinoic acid or vitamin D receptors as template). For dibenzoylhydrazines, numerous quantitative struc-

Table 3. *Literature data on interactions of EcRs and different ligands*

Compound	pI_{50}[a]	Literature[b]	Compound	pI_{50}[a]	Literature[b]
Ecdysone	D: 4.8–6.7	1–3	24-epi-Makisterone A (24S)	D: 6.7	4
20E	D: 6.2–8.1	2–10	Inokosterone, 25S	D: 6,6	3
20E	L: 6.5–7.0	11,12	Inokosterone, 25R	D: 6,8	3
20E	C: 6.4–6.6	11,12	Inokosterone	D: 6,4	9
Ponasterone A	D: 8.2–9.5	2,4,6,13	Shidasterone	D: 5,8	3
Ponasterone A	L: 8.2–8.7	11	20,26-Dihydroxy-ecdysone	D: <20E	14
Ponasterone A	C: 8.2	11	RH 5849	D: 5.4–6.2	5,6,15
Polypodine B	D: 9.0	4	RH 5849	L: 6.0–6.6	12
Turkesterone	D: 6.3	10	RH 5849	C: 6.1	12
Muristerone A	D: 8.2–8.5	9,10	RH 5992	D: 6.5–7.9	5,6
Malacosterone	D: 5.0	4	RH 5992	L: 7.5–9.0	11,12,16
25-OH-Atrotosterone A	D: 5.0	4	RH 5992	C: 4.9–5.9	11,12
Atrotosterone A	D: 7.6	4	8-O-Acetylharpagide	D: 4.0	7
Makisterone A (24R)	D: 7.9	4	DTBHIB	D: 5.2	8

[a] C = coleoptera; D = diptera; L = lepidoptera; pI_{50} = negative log of molar concentration needed for 50% effect.

[b] 1: Talbot et al. (1993); 2: Nakagawa et al. (1995); 3: Roussel et al. (1997); 4: Harmatha and Dinan (1997); 5: Mikitani et al. (1996); 6: Oikawa et al. (1994); 7: Elbrecht et al. (1996); 8: Mikitani et al. (1996); 9: Cottam and Milner (1997); 10: Spindler-Barth et al. (1997); 11: Dhadialla and Tzertzinis (1997); 12: Smagghe et al. (1996); 13: Cherbas et al. (1988); 14: Kayser et al. (1997); 15: Oikawa et al. (1994); 16: Thummel (1995).

ture activity relationship studies have been published, these data favor the orientation of RH5849 observed in the ECR model based on the VDR crystal structure, with the A-ring (Fig. 3D) oriented toward H5 and the β-sheet. Despite the ambiguity of the 20E orientation, both models suggest a similar superposition of 20E and RH5849. In the two RH5849/ECR-LBD complexes, the bulky *tert*-butyl group is oriented in the same groove. This superposition is unexpected and has never been proposed in previous studies (Fig. 3E,F). It provides a novel pharmacophore model that hopefully will give new ideas and stimulate the activity for the development of new synthetic ecdysone molecules.

Materials and methods

Generation of the protein model, ligand docking, and analysis of protein–ligand interactions

Models of the *C. tentans* ecdysone (ctECR) nuclear receptor LBD were first generated by homology with hRARγ or hVDR using the Modeller package (Sali & Blundell, 1993). The homology models are based on the sequence alignment shown in Figure 2 (aligned as described previously; Thompson et al., 1994) and using the hRARγ or hVDR crystal structure as a template. Ligands were positioned manually in each pocket using the probe-accessible and van der Waals volumes as guides; these volumes were generated with VOIDOO (Jones et al., 1991). The side chains in the vicinity of the ligand were positioned in favorable orientation using a rotamer library of the O package (Jones et al., 1991). Models were evaluated using stereochemical criteria (Procheck and ProsaII) and by visual inspection to score the 20E-derivatives and the synthetic ligands in a complex with the ECRra and ECRvd LBD (Fig. 1; Table 2). The Charmm package (QUANTA/CHARMM 98 package, Molecular Simulation Inc., Burlington, Massachusetts) was used for all the calculations. The ligand force field parameters used were those proposed by the Quanta/Charmm package.

The complexes were energy minimized in 2,000 steps with a dielectric constant of 4, using the Powell procedure. During the minimization process, the hydrogen bonds were defined by upper harmonic distance restraints (50 kcal/(mol Å)^2 force constant) and the overall structure of the LBD was maintained by harmonic position restraints (100 kcal/(mol Å)^2 force constant) of the Cα atoms of residues defining the secondary structure elements.

Conformational analyses of 20E and RH5849

Conformational analyses were done at the Hartree–Fock and DFT levels of theory using TURBOMOLE (Brode et al., 1993), which also permits to include solvent effects via the conductor-like screening model [COSMO (Klamt & Schüürmann, 1993)]. Triple zeta plus polarization (TZVP) basis sets were used throughout.

The 3D structure of 20E was derived from the X-ray structure of ecdysone (Huber & Hoppe, 1965) (HYCHLO code in the small molecule crystallographic database: CCSD), followed by a geometry optimization at the DFT level of theory. We also tried to find alternative conformations of the ecdysone tail, subject to the restriction that C-25 should be kept to its original position as close as possible. However, the energy of the lowest local minimum found was ~6 kcal/mol above the minimum structure actually used.

Conformational analyses of RH5992 with the MM2 force field came to the conclusion that in addition to the E,E X-ray conformation, a folded Z,E conformer should be considered in binding models (Fig. 3C,D, 4) (Hsu et al., 1997). Though not crucial to this discussion, the estimated MM2 barrier for the torsion around the N-N bond of ~5 kcal/mol appears to be too low. This can be inferred from a recent *ab initio* study on the rotational flexibility of diacylhydrazines which notes that the 180° barrier of N-methyl substituted hydrazines (12 kcal/mol) is as high as that of E,E-diformylhydrazine (Reynolds & Hormann, 1996). Our calculations support these findings. We investigated the torsion around the central N-N bond in RH5849 using RI-DFT (Brode et al., 1993) and the BP86 potential. The torsional angle Θ (C-N-N-C) was incremented by 15° steps from 0 to 360° and kept fixed while relaxing all other geometrical parameters. The resulting double-minimum potential (Fig. 4) with barriers of ~10 ($\Theta = 0°$) and ~18 kcal/mol ($\Theta = 180°$) has broad minima indicating some flexibility in Θ. As an example, the energy of the X-ray structure ($\Theta = -71.9°$) is only 0.01 kcal above the calculated minimum at $\Theta = -105°$.

The folded Z,E conformation of RH5849, comparable to conformation (1) of RH5992 in Hsu et al. (1997), is found to be 4.6 kcal/mol higher in energy. Actually, we do not find a stationary point similar to the Z,E conformation. Starting from almost coplanar phenyl rings, in the converged structure the planes of the phenyl rings build an angle of 125°. One might speculate that the reasons for this difference with respect to RH5992 are the missing hydrophobic interactions between the *para* ethyl group and the 3,5-dimethyl groups of the two phenyl rings. However, according to our DFT optimizations for both conformers of RH5992, its "folded" conformation adopts the same interphenyl angle of 125° and is again 5.1 kcal/mol higher in energy.

The energy difference between the *cis* and *trans* conformations of the *tert*-butyl-amide is 3.2 kcal/mol in favor of *cis*, while the corresponding rotational barrier is much higher. The optimized the *trans*-structure actually has an *tert*-butyl-N-C=O torsional angle of 146° and not of 180°, which would lead to an additional increase in energy. Taking into account the effect of bulk solvent by, for example, using COSMO, would modify the potential energy surface to some extent. However, the dielectric constant within a protein ($\epsilon \sim 4$) is more similar to vacuum than to water with $\epsilon = 78.4$. Hence, we are not allowed to reject some conformations because of their small stabilization energies.

In conclusion, for docking the dibenzoylhydrazines into the ligand-binding niche of the ECR, we are free to vary the N-N torsional angle Θ in the ranges of ($\pm$) 85 $\pm$ 40° affecting the conformational energy by <2 kcal/mol. We are, however, restricted not to alter the torsions around the amide bonds and hence to stay with the *E*,E overall conformation provided by the X-ray structures.

Acknowledgments

We thank Natacha Rochel, Isabelle Billas, and Graham Holmwood for critically reading the manuscript. This work was supported by funds from the Institut National de la Santé et de la Recherche Médicale, the Centre National de la Recherche Scientifique, the Hôspital Universitaire de Strasbourg, and BAYER AG. JF has benefited from a financial support from BAYER AG.

References

Barton GJ. 1993. ALSCRIPT: A tool to format multiple sequence alignments. *Protein Eng 6*:37–40.

Bourget W, Ruff M, Chambon P, Gronemeyer H, Moras D. 1995. Crystal structure of the ligand-binding domain of the human nuclear receptor RXR-a. *Nature 375*:377–382.

Brode S, Horn H, Ehrig M, Moldrup D, Rice JE, Ahlrichs R. 1993. Parallel direct SCF and gradient program for workstation clusters. *J Comput Chem 14*:1142–1148.

Brzozowski AM, Pike AC, Dauter Z, Hubbard RE, Bonn T, Engström O, Öhmann L, Greene GL, Gustafsson JA, Carlquist M. 1997. Molecular basis of agonism and antagonism in the oestrogen receptor. *Nature 389*:753–757.

Chan TH, Ali A, Britten JF, Thomas AW, Strunz GM, Salonius A. 1990. The crystal structure of 1,2-dibenzoyl-1-tert-butylhydrazine, a nonsteroidal ecdysone agonist, and its effect on spruce budworm (*Choristoneura fumiferana*). *Can J Chem 68*:1178–1181.

Cherbas P, Cherbas L, Lee SS, Nakanishi K. 1988. 26-[125I]Iodoponasterone A is a potent ecdysone and a sensitive radioligand for ecdysone receptors. *Proc Natl Acad Sci USA 85*:2096–2100.

Cho WL, Zapitskaya MZ, Raikhel AS. 1995. Mosquito ecdysteroid receptor: Analysis of the cDNA and expression during vitellogenesis. *Ins Biochem Molec Biol 25*:19–27.

Chung AC, Durica DS, Clifton SW, Roe BA, Hopkins PM. 1998. Cloning of crustacean ecdysteroid receptor and retinoid-X receptor gene homologs and elevation of retinoid-X receptor mRNA by retinoic acid. *Mol Cell Endocrinol 139*:209–227.

Cottam DM, Milner MJ. 1997. The effect of several ecdysteroids and ecdysteroid agonists on two Drosophila imaginal disk cell lines. *Cell Mol Life Sci 53*:600–603.

Cramer RD, Patterson DE, Bunce JD. 1989. Recent advances in comparative molecular field analysis (CoMFA). *Prog Clin Biol Res 291*:161–165.

Dhadialla TS, Tzertzinis G. 1997. Characterization and partial cloning of ecdysteroid receptor from a cotton boll weevil embryonic cell line. *Arch Insect Biochem Physiol 35*:45–57.

Elbrecht A, Chen Y, Jurgens T, Hensens OD, Zink DL, Beck HT, Balick MJ, Borris R. 1996. 8-O-Acetylharpagide is a nonsteroidal ecdysteroid agonist. *Ins Biochem Molec Biol 26*:519–523.

Evans SV. 1993. SETOR: Hardware lighted three-dimensional solid model representations of macromolecules. *J Mol Graphics 11*:134–138.

Fujiwara J, Jindra M, Newitt R, Palli SR, Hiruma K, Riddiford LM. 1995. Cloning of an ecdysone receptor homolog from *Manduca sexta* and the developmental profile of its mRNA in wings. *Ins Biochem Molec Biol 25*:845–856.

Gronemeyer H, Laudet V. 1995. Transcription factors 3: Nuclear receptors. *Protein Profile 2*:1173–1308.

Guo X, Harmon MA, Laudet V, Mangelsdorf DJ, Palmer MJ. 1998. Isolation of a functional ecdysteroid receptor homologue from the ixodid tick *Amblyomma americanum*. *Ins Biochem Molec Biol 27*:945–962.

Hannan GN, Hill RJ. 1997. Cloning and characterization of LcECR: A functional ecdysone receptor from the sheep blowfly *Lucilia cuprina*. *Ins Biochem Molec Biol 27*:479–488.

Harmatha J, Dinan L. 1997. Biological activity of natural and synthetic ecdysteroids in the BII bioassay. *Arch Insect Biochem Physiol 35*:219–225.

Hendlich M, Lackner P, Weitckus S, Floeckner H, Froschauer R, Gottsbacher K, Casari G, Sippl MJ. 1990. Identification of native protein folds amongst a large number of incorrect models. The calculation of low energy conformations from potentials of mean force. *J Mol Biol 216*:167–180.

Hsu AC, Fujimoto TT, Dhadialla TS. 1997. Structure-activity study and conformational analysis of RH-5992, the first commercialized nonsteroidal ecdysone agonist. *ACS Symp Ser 658*:206–219.

Huber R, Hoppe W. 1965. On the chemistry of ecdysone. VII. Analysis of the crystal and molecular structure of the molting hormone in insects, ecdysone, using the automized folding molecule method. *Chem Ber 98*:2403–2424.

Imhof MO, Rusconi S, Lezzi M. 1993. Cloning of a *Chironomus tentans* cDNA encoding a protein (cECRH) homologous to the *Drosophila melanogaster* ecdysteroid receptor (dECR). *Ins Biochem Molec Biol 23*:115–124.

Jepson I, Martinez A, Greenland AJ. 1996. A gene switch comprising an ecdysone receptor. *Inter Patent Applic WO 96/37609*.

Jones G, Sharp PA. 1997. Ultraspiracle: An invertebrate nuclear receptor for juvenile hormones. *Proc Natl Acad Sci USA 94*:499–413.

Jones TA, Zou JY, Cowan SW, Kjeldgaard. 1991. Improved methods for binding protein models in electron density maps and the location of errors in these models. *Acta Crystallogr A7*:110–119.

Kayser H, Winkler T, Spindler-Barth M. 1997. 26-Hydroxylation of ecdysteroids is catalyzed by a typical cytochrome P-450-dependent oxidase and related to ecdysteroid resistance in an insect cell line. *Eur J Biochem 248*:707–716.

Klamt A, Schüürmann G. 1993. COSMO: A new approach to dielectric screening in solvents with explicit expressions fot the screening energy and its gradient. *Perkin Trans 799*.

Kleywegt GJ, Jones TA. 1994. Detection, delineation, measurement and display of cavities in macromolecular structures. *Acta Crystallogr D50*:178–185.

Koelle MR, Talbot WS, Segraves WA, Bender MT, Cherbas P, Hogness DS. 1991. The Drosophila ECR gene encodes an ecdysone receptor, a new meber of the steroid receptor superfamily. *Cell 67*:59–77.

Kothapalli R, Palli SR, Ladd TR, Sohi SS, Cress D, Dhadialla TS, Tzertzinis G, Retnakaran A. 1995. Cloning and developmental expression of the ecdysone receptor gene from the spruce budworm, *Choristoneura fumiferana*. *Dev Genet 17*:319–330.

Lafont R. 1997. Ecdysteroids and related molecules in animals and plants. *Arch Insect Biochem Physiol 35*:3–20.

Laskowski RA, MacArthur MW, Moss DS, Thornton JM. 1993. PROCHECK: A program to check the stereochemical quality of proteins structures. *J Appl Crystallogr 26*:283–291.

Mikitani K. 1996. A new nonsteroidal chemical class of ligand for the ecdysteroid receptor 3, 5-di-tert-butyl-4-hydroxy-N-isobutyl-benzamide shows apparent insect molting hormone activities at molecular and cellular levels. *Biochem Biophys Res Com 227*:427–432.

Mohammed-Ali AK, Chan TH, Thomas AW, Strunz GM, Jewett B. 1995. Structure-activity relationship study of synthetic hydrazines as ecdysone agonists in the control of spruce budworm (*Choristoneura fumiferana*). *Can J Chem 73*:550–557.

Moras D, Gronemeyer H. 1999. The nuclear receptor ligand-binding domain: Structure and function. *Curr Opin Cell Biol 10*:384–391.

Mouillet JF, Delbecque JP, Quennedy B, Delachambre J. 1997. Cloning of two putative ecdysteroid receptor isoforms from Tenebrio molitor and their developmental expression in the epidermis during metamorphosis. *Eur J Biochem 248*:856–863.

Nakagawa Y, Shimizu B, Oikawa N, Akamatsu M, Nishimura K, Kurihara N, Ueno T, Fujita T. 1995. Three-dimensional quantitative structure-activity analysis of steroidal and dibenzoylhydrazine-type ecdysone agonists. *ACS Symp Ser 606*:288–301.

Nicholls A, Sharp KA, Honig B. 1991. Protein folding and association: Insights from the interfacial and thermodynamic properties of hydrocarbons. *Proteins 11*:281–296.

Nolte RT, Wisely GB, Westin S, Cobb JE, Lambert MH, Kurokawa R, Rosenfeld MG, Willson TM, Glass CK, Milburn MV. 1998. Ligand binding and co-activator assembly of the peroxisome proliferator-activated receptor-gamma. *Nature 395*:137–143.

Oikawa N, Nakagawa Y, Nishimura K, Ueno T, Fujita T. 1994a. Quantitative structure-activity analysis of larvicidal 1-(substituted benzoyl)-2-benzoyl-1-tert-butylhydrazines against *Chilo suppressalis*. *Pestic Sci 41*:139–148.

Oikawa N, Nakagawa Y, Nishimura K, Ueno T, Fujita T. 1994b. Quantitative structure-activity studies of insect growth regulators. X. Substituent effects on larvicidal activity of 1-tert-1-(2-chlorobenzoyl)-2-(substituted benzoyl-)hydrazines against *Chilo suppresalis* of potent derivatives. *Pest Biochem Physiol 48*:135–144.

Qian X. 1996. Molecular modeling study on the structure-activity relationship of substituted dibenzoyl-1-tert-butylhydrazines and their structural similarity to 20-hydroxyecdysone. *J Agric Food Chem 44*:1538–1542.

Renaud JP, Rochel N, Ruff M, Vivat V, Chambon P, Gronemeyer H, Moras D. 1995. Crystal structure of the RAR.gamma. ligand-binding domain bound to all-trans retinoic acid. *Nature 378*:681–689.

Reynolds CH, Hormann RE. 1996. Theoretical study of the structure and rotational flexibility of diacylhydrazines: Implications for the structure of nonsteroidal ecdysone agonists and azapeptides. *J Am Chem Soc 118*:395–391.

Rochel N, Wurtz JM, Mitschler A, Klaholz B, Moras D. 2000. Crystal structure of the nuclear receptor for vitamin D bound to its natural ligand. *Mol Cell 5*:173–179.

Roussel PG, Sik V, Turner NJ, Dinan LN. 1997. Synthesis and biological activity of side-chain analogs of ecdysone and 20-hydroxyecdysone. *J Chem Soc, Perkin Trans 1*:2237–2246.

Sali A, Blundell TL. 1993. Comparative protein modeling by satisfaction of spatial restraints. *J Mol Biol 234*:779–815.

Shiau AK, Barstad D, Loria PM, Cheng L, Kushner PJ, Agard DA, Greene GL. 1998. The structural basis of estrogen receptor/coactivator recognition and the antagonism of this interaction by tamoxifen. *Cell 95*:927–937.

Shimizu BI, Nakagawa Y, Hattori K, Nishimura K, Kurihara N, Ueno T. 1997. Molting hormonal and larvicidal activities of aliphatic acyl analogs of dibenzoylhydrazine insecticides. *Steroids 62*:638–642.

Smagghe G, Eelen H, Verschelde E, Richter K, Degheele D. 1996. Differential effects of nonsteroidal ecdysteroid agonists in Coleoptera and Lepidoptera: Analysis of evagination and receptor binding in imaginal disks. *Insect Biochem Mol Biol 26*:687–695.

Spindler-Barth M, Quack S, Rauch P, Spindler KD. 1997. Biological effects of muristerone A and turkesterone on the epithelial cell line from Chironomus tentans (D: Chironomidae) and correlation with binding affinity to the ecdysteroid receptor. *Eur J Entomol 94*:161–166.

Swevers L, Drevet JR, Lunke MD, Iatrou K. 1995. Cloning and analysis of

expression during follicular cell differentiation. *Ins Biochem Molec Biol 25*:857–866.

Talbot WS, Swyryd EA, Hogness DS. 1993. Drosophila tissues with different metamorphic responses to ecdysone express different ecdysone receptor isoforms. *Cell 73*:1323–1337.

Tanenbaum DM, Wang Y, Williams SP, Sigler PB. 1998. Crystallographic comparison of the estrogen and progesterone receptor's ligand binding domains. *Proc Natl Acad Sci USA 95*:5998–6003.

Thompson JD, Higgins DG, Gibson TJ. 1994. CLUSTAL W: Improving the sensitivity of progressive multiple sequence alignment through sequence weighting, position-specific gap penalties and weight matrix choice. *Nucleic Acids Res 22*:4673–4680.

Thummel CS. 1995. The regulation and function of Drosophila nuclear receptor superfamily members. *Cell 83*:871–877.

Thummel CS. 1996. Flies on steroids—Drosophila metamorphosis and the mechanism of steroid hormone action. *Trends in Genet 12*:306–310.

Wagner RL, Apriletti JW, McGrath ME, West BL, Baxter JD, Fletterick RJ. 1995. A structural role for hormone in the thyroid hormone receptor. *Nature 378*:690–697.

Williams SP, Sigler PB. 1998. Atomic structure of progesterone complexed with its receptor. *Nature 393*:392–396.

Wing KD, Slawecki RA, Carlson GR. 1988. RH5849, a nonsteroidal ecdysone agonist: Effects on larval Lepidoptera. *Science 241*:470–472.

Wurtz JM, Bourguet W, Renaud JP, Vivat V, Chambon P, Moras D, Gronemeyer H. 1996. A canonical structure for the ligand-binding domain of nuclear receptors. *Nat Struct Biol 3*:87–94.